

Chapter 5: Energy Decay in Isotropic Turbulence

Part 6: Limitations, shortcomings, and refinements

Scales of the turbulent motions provide a conceptual framework: energy cascade, vortex stretching, and Kolmogorov hypotheses. Some issues still under investigation, which are of interest. Conventional thinking is that these issues have limited impact for the study of practical turbulent flow applications since small scale motions $l < l_{EI}$ are thought to not directly influence the large-scale motion anisotropy and production of turbulence. However, this may not in fact be strictly true and these issues also have important implications for turbulence modeling.

The Reynolds number:

An important limitation of the Kolmogorov hypotheses is that they apply only for high Re , but a criterion for “sufficiently” high Re is not provided. Laboratory flows $Re \sim 10^4$ and $R_\lambda \sim 150$ show dissipative scales to be anisotropic. Note IIHR towing tank and wave basin usually use 3 m model with $Re \sim 5 \times 10^6$ ($Re_L \sim 2000$)

Experiments show that $E(\kappa) \sim \kappa^{-p}$, but the Kolmogorov -5/3 ($p = 1.7$) spectrum is approached slowly as Re increases $\rightarrow p = \frac{5}{3} - 8R_\lambda^{-3/4}$, such that for $R_\lambda = 200 \rightarrow p = 1.5$. Note $Re_L = \frac{3}{20}R_\lambda^2 \approx R_\lambda^2$.

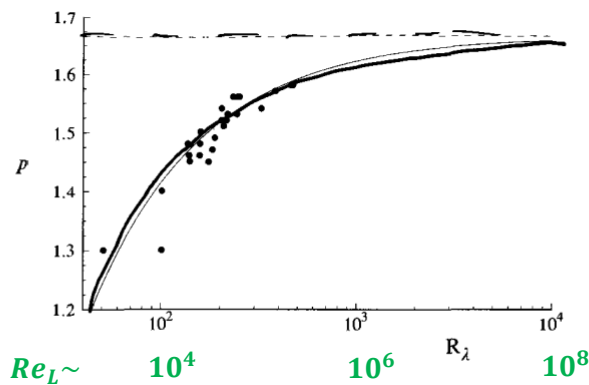


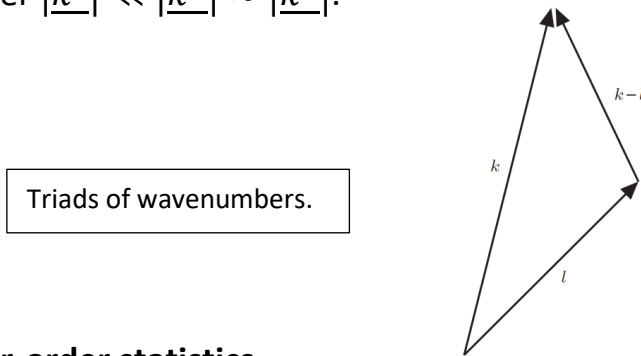
Fig. 6.29. The spectrum power-law exponent p ($E(\kappa) \sim \kappa^{-p}$) as a function of the Reynolds number in grid turbulence: symbols, experimental data of Mydlarski and Warhaft (1998); dashed line, $p = \frac{5}{3}$; solid line, empirical curve $p = \frac{5}{3} - 8R_\lambda^{-3/4}$.

DNS shows that energy transfer occurs not only from large to small l , but also from small to large l , with net transfer from the larger to the smaller scales.

In wave number space, as shown previously, the energy transfer is accomplished by triad interactions among modes:

$$\underline{\kappa}^a + \underline{\kappa}^b + \underline{\kappa}^c = 0$$

DNS results show that the transfer is predominantly local, with $|\underline{\kappa}^a| \approx |\underline{\kappa}^b|$, but that is affected by interactions with a third mode of significantly smaller wave number $|\underline{\kappa}^c| \ll |\underline{\kappa}^a| \approx |\underline{\kappa}^b|$.



Higher-order statistics

We have mostly (other than skewness S and palenstrophy G) considered only second order velocity statistics (i.e., statistics that are quadratic in velocity), which are of primary importance, e.g., as per the TKE k and Reynolds stresses $\langle u_i u_j \rangle$.

Simplest examples of higher-order statistics are the normalized velocity-derivative moments:

$$M_n = \overline{(u_{1,1})^n} / \overline{(u_{1,1})^2}^{n/2}$$

For $n = 3$ and $n = 4$, these are the velocity-derivative skewness S and kurtosis K .

$$M_3 = \overline{(u_{1,1})^3} / \overline{(u_{1,1})^2}^{3/2} = \text{Skewness } (S = 0 \text{ for Gaussian})$$

$S < 0 = f$ (vortex stretching and related energy transfer between scales) and measure of the bias or asymmetry in the velocity fluctuations between + and – values.

$$M_4 = \overline{(u_{1,1})^4} / \overline{(u_{1,1})^2}^2 = \text{Kurtosis } (K = 3 \text{ for Gaussian})$$

Measure of how much the velocity fluctuations are congregated at large and small values.

Kolmogorov originally assumed, the PDF of the velocity fluctuations is homogeneous and isotropic, which is often approximated as Gaussian, such that for each n , M_n is a constant; however, in fact, S and K are not constant but increase with Re .

Recall S (odd M_n) for $u_{1,1}$ plays a major role in the equation for the decay of isotropic turbulence, as does G (even M_n). Thus, non-Gaussian processes must be considered to predict the transfer term.

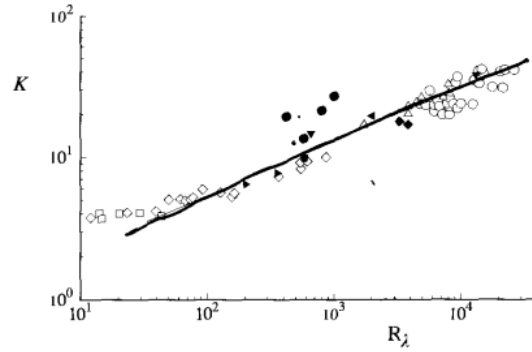
As shown in Part 1, S is related to the vortex stretching term in the ε equation and in Part 3 to the triple velocity correlation terms in the similarity form of the K-H equation. Fig. 6.32 compares the distribution of the normalized velocity derivative with a Gaussian distribution. The effect of the tails is fundamental to obtain a negative skewness, i.e., transfer of energy.

An equivalent definition of the skewness in wave number space is, which shows its relationship to the ratio of the Transfer term and energy spectrum:

$$S(t) = \frac{3\sqrt{30}}{14} \frac{\int_0^\infty k^2 T(k, t) dk}{\left[\int_0^\infty k^2 E(k, t) dk \right]^{3/2}} \quad \text{Appendix A.1}$$

$K \approx 4$ for low R_λ and $K \approx 40$ for high R_λ . Kurtosis does not reach an asymptotic value, but it increases as $\sim R_\lambda^{3/8}$. It is expected that K is related to G

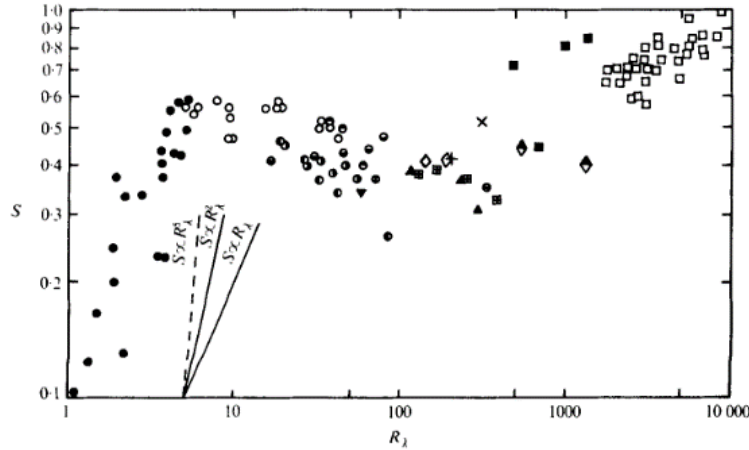
$$G = \frac{\overline{u^2 (u_{1,1})^2}}{\overline{(u_{1,1})^2}^2}$$



S and K are
very non-
Gaussian

Fig. 6.30. Measurements (symbols) compiled by Van Atta and Antonia (1980) of the velocity-derivative kurtosis as a function of Reynolds number. The solid line is $K \sim R_\lambda^{3/8}$.

For $R_\lambda < 10$, S decreases rapidly and it should go towards zero for $R_\lambda \ll 1$, as shown in Part 3. (k goes to zero like η^{-4} and is related to Skewness see page 14).



$S_k = 0.5$ was used
to solve $k - \varepsilon$
equations and K-H
equation.

FIGURE 1. Measurements of the velocity-derivative skewness in various turbulent flows plotted vs. the turbulent Reynolds number (see table 1 for symbols).

Type of flow	Author(s)	Symbol
Nearly isotropic grid turbulence	Batchelor & Townsend (1949)	●
	Stewart & Townsend (1951)	◐
	Mills <i>et al.</i> (1958)	◑
	Frenkiel & Klebanoff (1971)	◒
	Kuo & Corrsin (1971)	◓
	Betchov & Lorenzen (1974)	◔
	Bennett & Corrsin (1978)	○
	Present data	●
Homogeneous shear flow	Tavoularis (1978)	◊
Duct flow	Comte-Bellot (1965)	▲
	Elena, Chauve & Dumas (1977)	▼
Mixing layers	Wyngaard & Tennekes (1970)	+
	Champagne, Pao & Wygnanski (1976)	×
Axisymmetric jet	Friehe, Van Atta & Gibson (1972)	◆
	New measurements	◈
Boundary layer	Ueda & Hinze (1975)	◻
Atmosphere	Gibson, Stegen & Williams (1970)	■
	Wyngaard & Tennekes (1970)	□

TABLE 1

Higher order statistics pertaining to the inertial subrange are provided by the longitudinal velocity structure functions (Chapter 4 Part 8):

$$D_n(r) \equiv \overline{(\Delta_r u)^n}$$

Where:

$$\Delta_r u \equiv U_1(\underline{x} + \hat{e}_1 r, t) - U_1(\underline{x}, t)$$

Recall for the second (Chapter 4, Part 8) and third (Part 3, pg. 18) order structure functions $D_2(r)$, $D_3(r)$ in the inertial sub-range:

$$D_2 = D_{LL}(r, t) = C_2(\varepsilon r)^{2/3}$$

$$D_3 = D_{LLL}(r, t) = C_3 \varepsilon r$$

Which were determined according to Kolmogorov's second hypothesis, for $L \gg r \gg \eta$, $D_n(r)$ based on the assumption that they depend only on ε and r , i.e.,

$$D_n(r) \equiv \overline{(\Delta_r u)^n} = C_n(\varepsilon r)^{n/3}$$

Where C_n are constants ($C_2 = 2$, $C_3 = -4/5$).

More generally in the inertial subrange,

$$D_n(r) \sim r^{\zeta_n}$$

But the measured exponents differ from the Kolmogorov prediction, i.e., $\zeta_n = \frac{n}{3}$, as clearly $\zeta_n \neq \frac{n}{3}$ for $n \geq 4$.

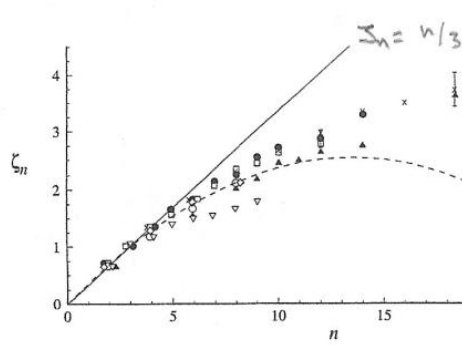
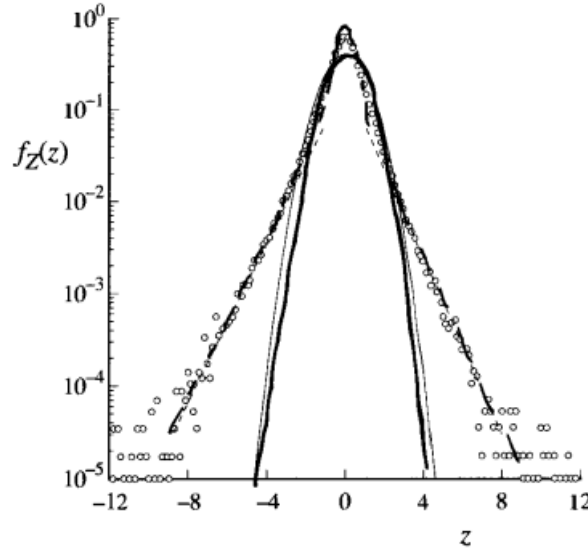


Fig. 6.31. Measurements (symbols) compiled by Anselmet *et al.* (1984) of the longitudinal velocity structure function exponent ζ_n in the inertial subrange, $D_n(r) \sim r^{\zeta_n}$. The solid line is the Kolmogorov (1941) prediction, $\zeta_n = \frac{1}{3}n$; the dashed line is the prediction of the refined similarity hypothesis, Eq. (6.323) with $\mu = 0.25$.

It is instructive to examine the PDFs that underlie M_n . For example, for $n=1$, the PDF is denoted by $f_Z(z)$, where Z is the standardized derivative

$$Z \equiv \frac{\partial u_1 / \partial x_1}{(u_{1,1})^2}^{1/2}$$

$$M_n \equiv 2 \int_0^\infty z^n f_Z(z) dz$$



$$M_1 = \frac{\overline{(\partial u_1 / \partial x_1)}}{(u_{1,1})^2}^{1/2}$$

Appendix A.2

Fig. 6.32. The PDF $f_Z(z)$ of the normalized velocity derivative $Z \equiv (\partial u_1 / \partial x_1) / (\overline{(\partial u_1 / \partial x_1)^2})^{1/2}$ measured by Van Atta and Chen (1970) in the atmospheric boundary layer (high Re). The solid line is a Gaussian; the dashed lines correspond to exponential tails (Eqs. (6.309) and (6.310)).

The tails of the distribution (beyond 4 SD) follow straight lines → exponential tails:

$$\begin{aligned} f_Z(z) &= 0.2 \exp(-1.1|z|), \quad \text{for } z > 4 \\ f_Z(z) &= 0.2 \exp(-1.0|z|), \quad \text{for } z < -4 \quad (0) \end{aligned}$$

Where the slower decay for negative z is consistent with $S < 0$. This clearly shows the importance of these rare events in the determination of S that has been shown to play a major role in the energy cascade.

The tails represent rare events: using (0) the probability of $|Z|$ exceeding 5 is equal to 0.3% (Appendix A.5).

$$P(-\infty \leq V \leq -5) + P(5 \leq V \leq \infty) = 2(F(\infty) - F(5)) = 2 \int_5^{\infty} f(V) dV$$

However, these low probability tails can make vast contributions to higher moments. For example, compare the tails for

$$M_n^{(5)} \equiv 2 \int_5^{\infty} z^n f_Z(z) dz$$

$$M_n \equiv 2 \int_0^{\infty} z^n f_Z(z) dz$$

Using (0) and considering only even moments so we can compare with Gaussian values.

Table 6.3. Contributions $M_n^{(5)}$ from the exponential tails ($|Z| > 5$) of the PDF of Z to the moments M_n according to Eqs. (6.310) and (6.311)

Moment n	Tail contribution $M_n^{(5)}$	Gaussian value M_n
0	0.003	1
2	0.1	1
4	4.2	3
6	220	15
8	1.5×10^4	105
10	1.4×10^6	945

The super skewness $M_6 = 220$, while Gaussian value is 15.

Dissipation intermittency

Discrepancies between M_n and $D_n(r)$ with EFD (i.e., non-Gaussian behavior) are attributed to the phenomenon of *internal intermittency* and accounted for in the *refined similarity hypotheses*, which introduces several new quantities related to dissipation.

Instantaneous dissipation

$$\varepsilon_0 = 2\nu s_{ij}s_{ij} \quad (1)$$

And

$$\varepsilon_r(\underline{x}, t) = \frac{3}{4\pi r^3} \iiint_{\forall(r)} \varepsilon_0(\underline{x} + \underline{r}, t) d\underline{r} \quad (2)$$

which represents the average of ε_0 within a sphere $\forall(r)$ of radius r .

One-dimensional surrogates for these quantities are represented by:

$$\begin{aligned} \hat{\varepsilon}_0 &= 15\nu \left(\frac{\partial u_1}{\partial x_1} \right)^2 \quad (2A) & \tilde{\varepsilon} &= 15\nu \overline{\left(\frac{\partial u_1}{\partial x_1} \right)^2} \\ \hat{\varepsilon}_r(x, t) &= \frac{1}{r} \int_0^r \hat{\varepsilon}_r(x + r, t) dr \end{aligned}$$

And in locally isotropic turbulence, each of these quantities have mean ε ,
i.e.,

$$\langle \hat{\varepsilon}_0 \rangle = \langle \hat{\varepsilon}_r(\underline{x}, t) \rangle = \varepsilon = \tilde{\varepsilon} \quad (2B)$$

$\hat{\varepsilon}_0$ intermittently attains high values.

R_λ laboratory (moderate) $\rightarrow \hat{\varepsilon}_0 / \varepsilon \approx 15$

R_λ atmosphere (high) $\rightarrow \hat{\varepsilon}_0 / \varepsilon \approx 50$

Kolmogorov conjectured that:

$$\frac{\overline{\hat{\varepsilon}_0^2}}{\varepsilon^2} \sim (L/\eta)^\mu$$

$$\frac{\overline{\hat{\varepsilon}_r^2}}{\varepsilon^2} \sim (L/r)^\mu$$

Where $L = k^{3/2}/\varepsilon$. For the inertial subrange, i.e., $\eta \ll r \ll L$ and $\mu > 0 =$ constant=intermittency exponent. Note above equations are for mean square $\hat{\varepsilon}_0$ and $\hat{\varepsilon}_r$.

EFD for $\frac{\overline{\hat{\varepsilon}_r^2}}{\varepsilon^2}$ shows $\mu = 0.25 \pm 0.05$.

Note that $\overline{\hat{\varepsilon}_0^2}/\varepsilon^2 = K$ (as shown later) and for $\mu = 0.25$, and recalling that $L/\eta \sim R_\lambda^{3/4}$:

$$K \sim R_\lambda^{3\mu/2} = R_\lambda^{3/8}$$

Which is consistent with EFD shown in Fig. 6.30. Recall discussion Chapter 4 Part 6 pg. 19 that bottleneck effect and departure small-scale turbulence from -5/3 law related to ε intermittency.

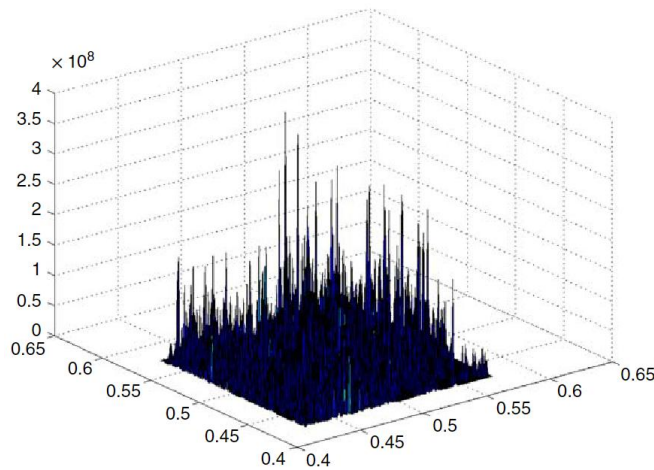


Figure 4.9 Dissipation rate on a plane showing intermittency within a region of isotropic turbulence computed in a vortex filament simulation of flow in a periodic box.

Refined similarity hypotheses

Original first hypothesis: $\Delta_r u$ for $r \ll L$ are universal and $f(\varepsilon, \nu)$.

Refined first hypothesis: $\Delta_r u$ for $r \ll L$ are universal and $f(\varepsilon_r, \nu)$.

Refined second hypothesis: $\Delta_r u$ for $\eta \ll r \ll L$ are universal and $f(\varepsilon_r)$.

The structure functions in the inertial subrange are:

$$D_n(r) = \langle (\Delta_r u)^n \rangle = \langle C_n (\varepsilon r)^{n/3} |_{\varepsilon=\varepsilon_r} \rangle = C_n \langle \varepsilon_r^{n/3} \rangle r^{n/3}$$

Where C_n are universal constants and ε_r is a volume averaged variable, as per $\hat{\varepsilon}_r(x, t)$.

For $n = 3$, since $\overline{\varepsilon_r} = \varepsilon$, the original and the refined hypotheses make the same prediction, i.e., $C_3 = -4/5$, which represents the Kolmogorov 4/5 law.

For $n = 6$, using

$$\frac{\overline{\hat{\varepsilon}_r^2}}{\varepsilon^2} \sim (L/r)^\mu$$

Such that

$$D_6(r) = C_6 \langle \varepsilon_r^{6/3} \rangle r^{6/3} = C_6 \langle \varepsilon_r^2 \rangle r^2 \sim \varepsilon^2 L^\mu r^{2-\mu}$$

A power law in r as per $D_n(r) \sim r^{\zeta_n}$ with $\zeta_6 = 2 - \mu = 1.75$ for $\mu = 0.25$. (See Fig. 6.31)

For other n , $\overline{\varepsilon_r^{n/3}}$ can be determined from the PDF of ε_r , which is assumed to be log-normally distributed, i.e., $\ln(\varepsilon_r/\varepsilon_{ref})$ has Gaussian distribution such that:

$$\frac{\overline{\varepsilon_r^n}}{\overline{\varepsilon_r^n}} \sim (L/r)^{n(n-1)\mu/2} \quad (3)$$

Pope Ex 6.37
Appendix A.3

Consequently, if the structure function is predicted to scale as $D_n(r) \sim r^{\zeta_n}$,

$$\begin{aligned}
 D_n(r) &= C_n \langle \varepsilon_r^{\frac{n}{3}} \rangle r^{\frac{n}{3}} \\
 &= C_n \overline{\varepsilon_r}^{n/3} (L/r)^{n(n/3-1)\mu/6} r^{n/3} \\
 &= C_n \overline{\varepsilon_r}^{n/3} L^{n(n-1)\mu/6} r^{\frac{n/3 - n(n/3-1)\mu/6}{\zeta_n}}
 \end{aligned}$$

$$\zeta_n = \frac{1}{3}n \left[1 - \frac{1}{6}\mu(n-3) \right]$$

For $n \leq 10$, this prediction is in reasonable agreement with Fig. 6.31. For large n , the large errors are due to the assumption of the log-normal distribution.

For $D_2(r)$:

$$\zeta_2 = \frac{2}{3} + \frac{1}{9}\mu \approx \frac{2}{3} + \frac{1}{36}$$

Applying a Fourier transform to $D_n(r)$ Appendix A.4 results in an expression for the energy spectrum in the inertial range of the form:

$$E(k) = A \overline{\varepsilon_r}^{\frac{n}{3}} k^{-\frac{5}{3}} (Lk)^{-\mu}$$

This shows that in the inertial-range the spectrum is predicted to be a power law $E(k) \sim k^{-p}$ with

$$p = \frac{5}{3} + \frac{1}{9}\mu \approx \frac{5}{3} + \frac{1}{36}$$

Hence, only small correction to the -5/3 spectrum.

For the velocity-derivative moments, using Eq. (2A)

$$\left(\frac{\partial u_1}{\partial x_1}\right)^2 = \frac{\hat{\varepsilon}_0}{15\nu}$$

And for a general exponent n

$$\left(\frac{\partial u_1}{\partial x_1}\right)^n = \left(\frac{\hat{\varepsilon}_0}{15\nu}\right)^{n/2} = C_n \left(\frac{\hat{\varepsilon}_0}{\nu}\right)^{n/2}$$

Using the refined hypotheses (Eq. 2B) yield

$$\overline{(u_{1,1})^n} = \overline{C_n} \left(\frac{\overline{\varepsilon_r}}{\nu}\right)^{n/2}$$

With $\overline{C_n} = \text{constants}$, and hence

$$M_n = \frac{\overline{(u_{1,1})^n}}{\overline{(u_{1,1})^2}^{n/2}} = \frac{\overline{C_n} \left(\frac{\overline{\varepsilon_r}}{\nu}\right)^{\frac{n}{2}}}{\left(\overline{C_2} \left(\frac{\overline{\varepsilon_r}}{\nu}\right)\right)^{n/2}} = \frac{\overline{C_n} \overline{\varepsilon_r}^{n/2}}{(\overline{C_2} \overline{\varepsilon_r})^{n/2}} \quad (4)$$

Substituting Eq. (3) into Eq. (4) for $n = 3$ (S) and $n = 4$ (K):

$$M_3 = \frac{\overline{C_n} \overline{\varepsilon_r}^{3/2}}{(\overline{C_2} \overline{\varepsilon_r})^{3/2}} = \frac{\overline{C_n}}{(\overline{C_2})^{3/2}} (L/r)^{3/2(3/2-1)\mu/2} = \frac{\overline{C_n}}{(\overline{C_2})^{3/2}} (L/r)^{3\mu/8}$$

$$M_4 = \frac{\overline{C_n} \overline{\varepsilon_r}^{4/2}}{(\overline{C_2} \overline{\varepsilon_r})^{4/2}} = \frac{\overline{C_n}}{(\overline{C_2})^{3/2}} (L/r)^{2(2-1)\mu/2} = \frac{\overline{C_n}}{(\overline{C_2})^{3/2}} (L/r)^\mu$$

$$-S \sim (L/r)^{3\mu/8}$$

$$K \sim (L/r)^\mu$$

Hence

$$-S \sim K^{3/8}$$

Which is consistent with EFD:

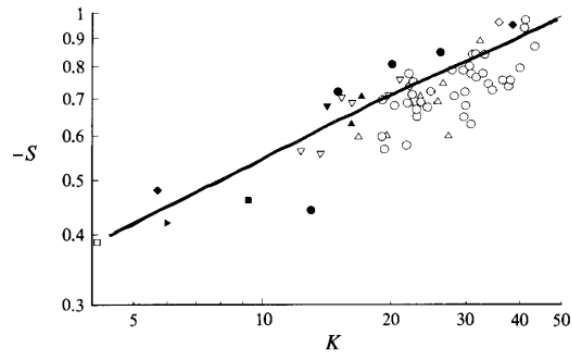


Fig. 6.33. Measurements of the velocity-derivative skewness S and kurtosis K compiled by Van Atta and Antonia (1980). The line is $-S \sim K^{3/8}$.

Appendix A

A.1

Definition of Skewness of $u_{1,1}$:

$$S(t) = -\frac{\overline{(u_{1,1})^3}}{\overline{(u_{1,1})^2}^{3/2}} \quad (1A)$$

Using the relation obtained in Chapter 4 Part 3:

$$\overline{u^2} f''(0) = -\overline{u_{1,1}^2} \quad (2A)$$

And substituting Eq. (2A) into (1A) gives

$$S(t) = \frac{\overline{(u_{1,1})^3}}{\left(\overline{u^2} f''(0)\right)^{\frac{3}{2}}} \quad (3A)$$

Next, the relation between $f''(0)$ and ε is given by

$$\varepsilon = -15\nu \overline{u^2} f''(0) \rightarrow f''(0) = -\frac{\varepsilon}{15\nu \overline{u^2}} \quad (4A)$$

Substituting Eq. (4A) into (3A) yields

$$S(t) = \frac{\overline{(u_{1,1})^3}}{\left(\overline{u^2} f''(0)\right)^{\frac{3}{2}}} = -\frac{\overline{(u_{1,1})^3}}{\left(\overline{u^2} \frac{\varepsilon}{15\nu \overline{u^2}}\right)^{\frac{3}{2}}} = -\frac{\overline{(u_{1,1})^3}}{\left(\frac{\varepsilon}{15\nu}\right)^{\frac{3}{2}}} \quad (5A)$$

Where ε can be related to the 3D energy spectrum using

$$\varepsilon = 2\nu \int_0^\infty \kappa^2 E(\kappa, t) d\kappa \quad (6A)$$

And substituting Eq. (6A) into (5A) gives

$$S = - \frac{\overline{(u_{1,1})^3}}{\left(\frac{2\nu \int_0^\infty \kappa^2 E(\kappa, t) d\kappa}{15\nu} \right)^{\frac{3}{2}}} = - \left(\frac{15}{2} \right)^{3/2} \frac{\overline{(u_{1,1})^3}}{\left(\int_0^\infty \kappa^2 E(\kappa, t) d\kappa \right)^{\frac{3}{2}}} \quad (7A)$$

Next, $\overline{(u_{1,1})^3}$ can be related to $k'''(0)$ as shown in Chapter 4 Part 2

$$\overline{(u_{1,1})^3} = S_{11,1} = u_{rms}^3 k'''(0) \quad (8A)$$

Moreover, in Chapter 5 Part 4 the quantity $S_{i,i}$ was defined as

$$S_{ii}(\underline{r}, t) = \frac{\partial S_{ik,i}}{\partial r_k}(-\underline{r}, t) + \frac{\partial S_{ik,i}}{\partial r_k}(\underline{r}, t)$$

Or equivalently $rS_{i,i}(r, t)$ is the Fourier transform of $T(k, t)/k$ where $T(k, t)$ is the transfer term:

$$S_{i,i}(r, t) = 2 \int_0^\infty \frac{\sin kr}{kr} T(k, t) dk \quad (9A)$$

Next, $\sin(kr)$ can be approximated using a Taylor series expansion as:

$$\sin(kr) = kr - \frac{\kappa^3 r^3}{6} + O(r^5)$$

Such that Eq. (9A) becomes:

$$\begin{aligned} S_{i,i}(r, t) &= 2 \int_0^\infty \frac{\left(kr - \frac{\kappa^3 r^3}{6}\right)}{kr} T(k, t) dk \\ &= 2 \int_0^\infty \left(1 - \frac{\kappa^2 r^2}{6}\right) T(k, t) dk \\ &= 2 \int_0^\infty T(k, t) dk - 2 \int_0^\infty \left(\frac{\kappa^2 r^2}{6}\right) T(k, t) dk \end{aligned}$$

Where the first term on the RHS is zero in view of the reasoning shown in Chapter 5 Part 4.

$$S_{i,i}(r, t) = - \int_0^\infty \left(\frac{\kappa^2 r^2}{3}\right) T(k, t) dk \quad (10A)$$

Isolating $\int_0^\infty \kappa^2 T(k, t) dk$ on the RHS of Eq. (10A) gives

$$\frac{3}{r^2} S_{i,i}(r, t) = - \int_0^\infty \kappa^2 T(k, t) dk \quad (11A)$$

In Appendix A.7 of Chapter 5 Part 4 it was shown that:

$$S_{ii}(r, t) = \frac{35}{6} u_{rms}^3 r^2 k'''(0, t) \quad (12A)$$

Substituting Eq. (12A) into (11A) yields

$$\begin{aligned}\frac{3}{r^2} \frac{35}{6} u_{rms}^3 r^2 k'''(0, t) &= - \int_0^\infty \kappa^2 T(k, t) dk \\ \frac{35}{2} u_{rms}^3 k'''(0) &= - \int_0^\infty \kappa^2 T(k, t) dk \\ k'''(0) &= - \frac{2}{35 u_{rms}^3} \int_0^\infty \kappa^2 T(k, t) dk \quad (13A)\end{aligned}$$

Substituting Eq. (13A) in the RHS of Eq. (8A) gives

$$\overline{(u_{1,1})^3} = u_{rms}^3 k'''(0) = - \frac{2}{35} \int_0^\infty \kappa^2 T(k, t) dk \quad (14A)$$

Finally, substituting Eq. (14A) into (7A) an expression for $S(t)$ as a function of the transfer term and the energy spectrum is obtained:

$$S(t) = - \left(\frac{15}{2} \right)^{3/2} \frac{\overline{(u_{1,1})^3}}{\left(\int_0^\infty \kappa^2 E(\kappa, t) d\kappa \right)^{3/2}} = \frac{2}{35} \left(\frac{15}{2} \right)^{3/2} \frac{\int_0^\infty \kappa^2 T(k, t) dk}{\left(\int_0^\infty \kappa^2 E(\kappa, t) d\kappa \right)^{3/2}}$$

$$\frac{2}{35} \left(\frac{15}{2} \right)^{3/2} = \frac{2}{7} \frac{3}{2} \sqrt{\frac{15}{2}} \sqrt{\frac{2}{2}} = \frac{3}{14} \sqrt{30}$$

$$S(t) = \frac{3}{14} \sqrt{30} \frac{\int_0^\infty \kappa^2 T(k, t) dk}{\left(\int_0^\infty \kappa^2 E(\kappa, t) d\kappa \right)^{3/2}}$$

A.2

1. Probability Density Function (PDF) $f_Z(z)$

The function $f_Z(z)$ represents the probability density function (PDF) of the standardized velocity derivative Z . It describes the statistical distribution of Z , meaning it provides the likelihood of different values occurring in turbulent flow.

Mathematically, if Z is a random variable, then $f_Z(z)$ satisfies:

$$P(a \leq Z \leq b) = \int_a^b f_Z(z) dz \quad (1)$$

which means that the integral of $f_Z(z)$ over an interval $[a, b]$ gives the probability that Z falls within that range.

2. Standardized Velocity Derivative Z

The quantity Z is defined as:

$$Z \equiv \frac{u_{1,1}}{\left(\overline{(u_{1,1})^2}\right)^{1/2}} \quad (2)$$

where:

- $u_{1,1} = \frac{\partial u_1}{\partial x_1}$ is the velocity gradient.
- The denominator is the standard deviation of $u_{1,1}$, ensuring that Z has zero mean and unit variance.

3. Statistical Moment M_1

The moment M_1 is defined as:

$$M_1 = \frac{\overline{(u_{1,1})^1}}{\left(\overline{(u_{1,1})^2}\right)^{1/2}} \quad (3)$$

which represents the mean of $u_{1,1}$ normalized by its standard deviation.

Since Z is defined as a standardized form of $u_{1,1}$, we can rewrite M_1 as:

$$M_1 = \overline{Z} \quad (4)$$

which means that M_1 is simply the mean of the standardized variable Z . If $f_Z(z)$ is symmetric around zero (as in a Gaussian distribution), then $M_1 = 0$, indicating no preferred direction for velocity gradient fluctuations. However, real turbulence often exhibits nonzero M_1 due to intermittency effects.

4. Final Relationship

The first statistical moment M_1 is computed directly from the PDF $f_Z(z)$ as:

$$M_1 = \int_{-\infty}^{\infty} z f_Z(z) dz. \quad (5)$$

Thus, $f_Z(z)$ describes the distribution of Z , and M_1 is derived from $f_Z(z)$ as its first moment.

A.3

Turbulent Flows
Stephen B. Pope
Cambridge University Press (2000)

Solution to Exercise 6.37

Prepared by: Timo de Ruijscher

Date: 01/11/2017

- a) According to Exercise 3.7, the raw moments of log-normally distributed stochastic variable Y are given by Eq.(3.52)

$$\langle Y^n \rangle = \exp \left(n\mu + \frac{1}{2}n^2\sigma^2 \right). \quad (1)$$

The log-normal nature of ε_r as given by Eq.(6.331) can be rewritten as

$$\frac{\varepsilon_r}{\varepsilon_{\text{ref}}} = e^\phi, \quad (2)$$

with $\phi \sim \mathcal{N}(\langle \phi \rangle, \sigma^2)$. From Eq.(2) the moments of ε_r are calculated as

$$\frac{1}{\varepsilon_{\text{ref}}^n} \langle \varepsilon_r^n \rangle = \left\langle \left(\frac{\varepsilon_r}{\varepsilon_{\text{ref}}} \right)^n \right\rangle = \exp \left(n \langle \phi \rangle + \frac{1}{2}n^2\sigma^2 \right), \quad (3)$$

which is rewritten as

$$\langle \varepsilon_r^n \rangle = \varepsilon_{\text{ref}}^n \exp \left(n \langle \phi \rangle + \frac{1}{2}n^2\sigma^2 \right). \quad (4)$$

- b) After substituting $\varepsilon = \langle \varepsilon_r \rangle$ and $n = 1$ in Eq.(4) it follows that

$$\langle \varepsilon_r \rangle = \varepsilon_{\text{ref}} \exp \left(\langle \phi \rangle + \frac{1}{2}\sigma^2 \right), \quad (5)$$

resulting in $\langle \phi \rangle = -\frac{1}{2}\sigma^2$. Substituting this result again with $\varepsilon = \langle \varepsilon_r \rangle$ in Eq.(4), the final expression follows as

$$\begin{aligned}\frac{\langle \varepsilon_r^n \rangle}{\langle \varepsilon_r \rangle^n} &= \exp \left(-\frac{1}{2}n\sigma^2 + \frac{1}{2}n^2\sigma^2 \right) \\ &= \exp \left[\frac{1}{2}\sigma^2 n(n-1) \right].\end{aligned}\quad (6)$$

- c) Substituting $n = 2$ in Eq.(6), it follows for the second order moment of ε_r that

$$\frac{\langle \varepsilon_r^2 \rangle}{\langle \varepsilon_r \rangle^2} = \exp(\sigma^2) \equiv A \left(\frac{L}{r} \right)^\mu. \quad (7)$$

The result of Eq.(7) can be solved for σ^2 as

$$\begin{aligned}\sigma^2 &= \ln \left[A \left(\frac{L}{r} \right)^\mu \right] \\ &= \ln A + \ln \left[\left(\frac{L}{r} \right)^\mu \right] \\ &= \ln A + \mu \ln \left(\frac{L}{r} \right).\end{aligned}\quad (8)$$

Finally, by substituting Eq.(8) into Eq.(6), it follows for the n^{th} order raw moments of ε_r that

$$\begin{aligned}\frac{\langle \varepsilon_r^n \rangle}{\langle \varepsilon_r \rangle^n} &= \exp \left[\frac{1}{2} \left(\ln A + \mu \ln \left(\frac{L}{r} \right) \right) n(n-1) \right] \\ &= \exp \left[\frac{1}{2} n(n-1) \ln A + \frac{1}{2} n(n-1) \mu \ln \left(\frac{L}{r} \right) \right] \\ &= \exp \left[\ln \left(A^{n(n-1)/2} \right) + \ln \left(\frac{L}{r} \right)^{\mu n(n-1)/2} \right] \\ &= A^{n(n-1)/2} \left(\frac{L}{r} \right)^{\mu n(n-1)/2}.\end{aligned}\quad (9)$$

A.4

Derivation of the Energy Spectrum $E(k)$

Step 1: Definition of the Structure Function

The second-order velocity structure function is defined as:

$$D_2(r) = \langle (\delta u_r)^2 \rangle \sim r^{\zeta_2}$$

where $\delta u_r = u(x+r) - u(x)$ is the velocity difference across a separation r . The scaling law assumes that in the inertial range of turbulence, the structure function behaves as:

$$D_2(r) \sim r^{\zeta_2}.$$

From the given text, we have:

$$\zeta_2 = \frac{2}{3} + \frac{1}{9}\mu.$$

Our goal is to derive the corresponding power-law form of the **energy spectrum** $E(k)$.

Step 2: Fourier Transform Relation

The energy spectrum $E(k)$ is related to the velocity correlation function via a Fourier transform. The two-point velocity correlation function is:

$$R_{ij}(r) = \langle u(x)u(x+r) \rangle.$$

The energy spectrum $E(k)$ is obtained from the Fourier transform of $R_{ij}(r)$:

$$E(k) = \int R_{ij}(r) e^{-ikr} dr.$$

Since the structure function $D_2(r)$ and the correlation function $R_{ij}(r)$ are related as:

$$D_2(r) = 2(R_{ij}(0) - R_{ij}(r)),$$

and given that in the inertial range $D_2(r) \sim r^{\zeta_2}$, it follows that:

$$R_{ij}(r) \sim r^{\zeta_2}.$$

Step 3: Dimensional Analysis and Scaling

To find the corresponding energy spectrum, we use **dimensional analysis** and the fact that a function $R_{ij}(r) \sim r^{\zeta_2}$ has a Fourier transform that scales as:

$$E(k) \sim k^{-(\zeta_2+1)}.$$

This follows from the general property that the Fourier transform of a power-law function r^α results in a power-law function in k with exponent $-\alpha - 1$:

$$\mathcal{F}[r^\alpha] \sim k^{-\alpha-1}.$$

Since $R_{ij}(r) \sim r^{\zeta_2}$, the energy spectrum behaves as:

$$E(k) \sim k^{-(\zeta_2+1)}.$$

Step 4: Applying the Known Value of ζ_2

From the given equation:

$$\zeta_2 = \frac{2}{3} + \frac{1}{9}\mu.$$

Using the relation $E(k) \sim k^{-(\zeta_2+1)}$, we obtain:

$$p = \zeta_2 + 1 = \frac{2}{3} + \frac{1}{9}\mu + 1.$$

Simplifying:

$$p = \frac{5}{3} + \frac{1}{9}\mu.$$

Approximating $\frac{1}{9}\mu \approx \frac{1}{36}$, we get:

$$p \approx \frac{5}{3} + \frac{1}{36}.$$

Thus, the final power-law form of the energy spectrum is:

$$E(k) \sim k^{-p} \quad \text{where} \quad p = \frac{5}{3} + \frac{1}{36}.$$

Conclusion

The Fourier transform provides the key link between the velocity structure function and the energy spectrum. The exponent in the power law of $E(k)$ is determined as:

$$p = \zeta_2 + 1.$$

Since the classical Kolmogorov theory predicts $p = 5/3$, the intermittency correction $\frac{1}{36}$ slightly modifies the spectrum, but the deviation is small.

A.5

Characterization of random variables

$$p = P(B) = P(U < V_b)$$

$$0 \leq p \leq 1$$

0=impossible, 1=sure thing

CDF = Cumulative Distribution function = $F(V) = P(U < V)$ or $P(B) = P(U < V_b) = F(V_b)$

$$F(-\infty) = 0 \text{ since } (U < -\infty) = 0$$

Also $F(V_b) > F(V_a)$ for $V_b > V_a$ since $p > 0$

$$F(\infty) = 1 \text{ since } (U < \infty) = 1$$

$$F(V_b) - F(V_a) = P(V_a \leq U \leq V_b) > 0$$

CDF is non-decreasing function.

PDF = Probability Density function

$$f(V) = \frac{dF(V)}{dV} \geq 0$$

$$\int_{-\infty}^{\infty} f(V)dV = 1$$

$$f(-\infty) = f(\infty) = 0$$

$$P(V_a \leq V \leq V_b) = F(V_b) - F(V_a) = \int_{V_a}^{V_b} f(V)dV$$

$$P(V \leq U \leq V + dV) = F(V + dV) - F(V) = f(V)dV$$

$$\frac{\Delta F}{dV} = f(V)$$

Probability per unit distance

PDF has dimensions U^{-1} .

CDF and $f(V)dV$ are non-dimensional.

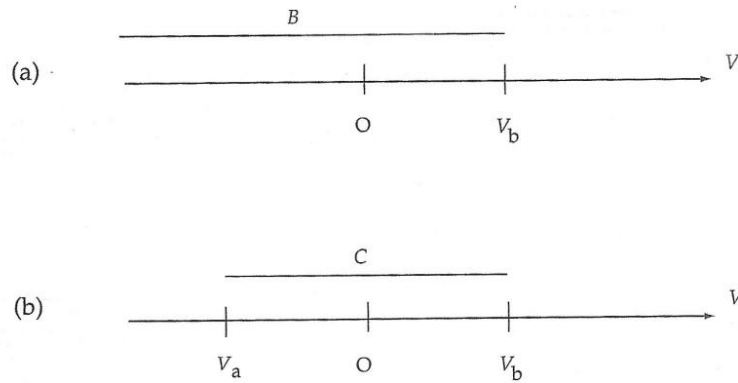


Fig. 3.3. Sketches of the sample space of U showing the regions corresponding to the events (a) $B \equiv \{U < V_b\}$, and (b) $C \equiv \{V_a \leq U < V_b\}$.

Sample space: $B = (U < V_b)$, $C = (V_a \leq U < V_b)$ for $V_a < V_b$.

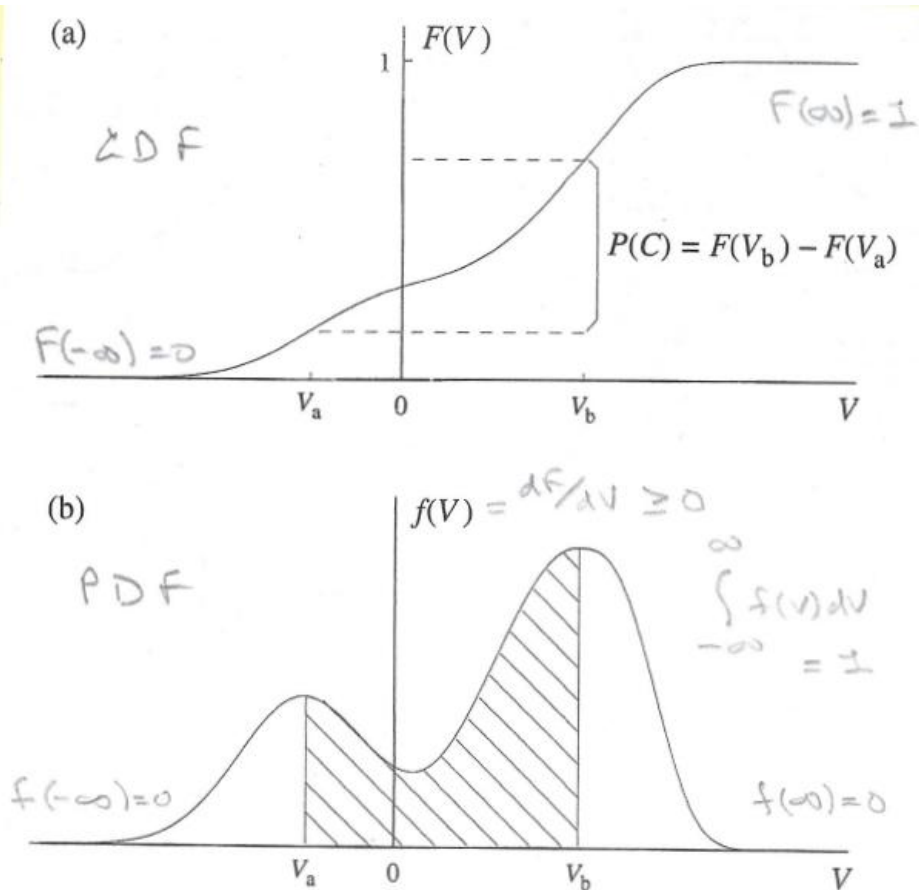


Fig. 3.4. Sketches of (a) the CDF of the random variable U showing the probability of the event $C \equiv \{V_a \leq U < V_b\}$, and (b) the corresponding PDF. The shaded area in (b) is the probability of C .

Means and moments.

Mean or expectation or EV of U :

$$\bar{U} = \int_{-\infty}^{\infty} V f(V) dV$$

Represents the probability weighted average over all values U .

EV of $Q(U)$:

$$\overline{Q(U)} = \int_{-\infty}^{\infty} Q(V) f(V) dV$$

Properties:

$$\overline{[aQ(U) + bR(U)]} = a\overline{Q(U)} + b\overline{R(U)}$$

$$\overline{\bar{U}} = \bar{U}$$

Fluctuation in U : $u = U - \bar{U}$

Variance of U :

$$\text{var}(U) \equiv \overline{u^2} = \int_{-\infty}^{\infty} (V - \bar{U})^2 f(V) dV$$

Standard deviation of U :

$$\text{SD}(U) = \sqrt{\text{var}(U)} = \sqrt{\overline{u^2}} = \text{rms} = u' = \sigma_u$$

nth central moment:

$$\mu_n = \overline{u^n} = \int_{-\infty}^{\infty} (V - \bar{U})^n f(V) dV$$

Where $\mu_0 = 1$, $\mu_1 = 0$, $\mu_2 = \sigma_u^2$

Standardization

It is often convenient to work with standardized random variables, which, by definition, have zero mean and unit variance.

$$\hat{U} = \frac{(U - \bar{U})}{\sigma_u} = \frac{u}{\sigma_u} = \frac{u}{\sqrt{\overline{u^2}}}$$

The PDF of \hat{U} is:

$$\hat{f}(\hat{V}) = \sigma_u f(\bar{U} + \sigma_u \hat{V})$$

The moments of \hat{U} are:

$$\hat{\mu}_n = \frac{\overline{\mu_n}}{\sigma_u^n} = \frac{\mu_n}{\sigma_u^n} = \int_{-\infty}^{\infty} \hat{V}^n \hat{f}(\hat{V}) d\hat{V}$$

Where $\hat{\mu}_0 = 1$, $\hat{\mu}_1 = 0$, $\hat{\mu}_2 = 1$. The third standardized moment $\hat{\mu}_3$ is called the skewness, and the fourth $\hat{\mu}_4$ is the flatness or kurtosis.

Examples of probability distributions

Uniform distribution

$U = \text{uniform for } a \leq V < b$

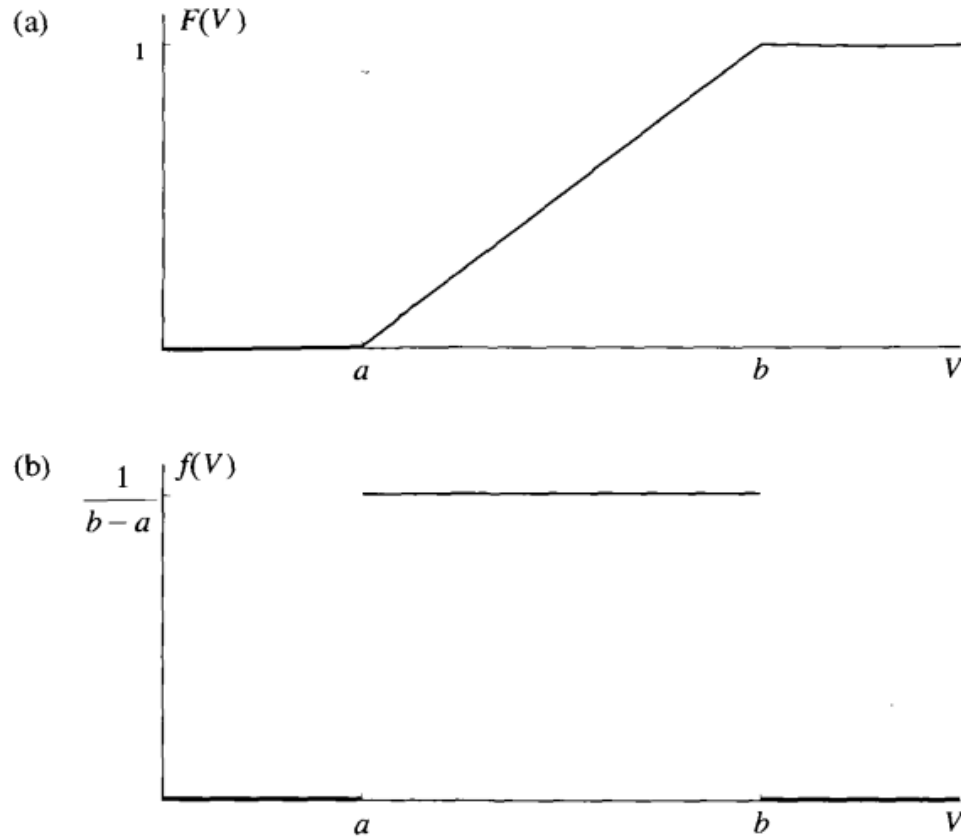


Fig. 3.5. The CDF (a) and the PDF (b) of a uniform random variable (Eq. (3.39)).

$$f(V) = \begin{cases} \frac{1}{b-a}, & \text{for } a \leq V < b, \\ 0, & \text{for } V < a \text{ and } V \geq b \end{cases}$$

$$c = a \leq V < b$$

$$P(c) = F(b) - F(a) \geq 0$$

$$f(V) = \frac{dF(V)}{dV}$$

The normal distribution

U normal with $EV=\mu$ and $SD=\sigma$.

PDF

$$f(V) = \mathcal{N}(V; \mu, \sigma^2) = \frac{1}{\sigma\sqrt{2\pi}} \exp\left[-\frac{1}{2}(V - \mu)^2/\sigma^2\right]$$

We can standardize U if it is normally distributed:

$$\hat{U} \equiv (U - \mu)/\sigma$$

And the corresponding PDF is:

$$\hat{f}(V) = \mathcal{N}(V; 0, 1) = \frac{1}{\sqrt{2\pi}} e^{-V^2/2}$$

The corresponding CDF is:

$$\hat{F}(V) = \int_{-\infty}^V \frac{1}{\sqrt{2\pi}} e^{-x^2/2} dx = \frac{1}{2} [1 + \operatorname{erf}(V/\sqrt{2})]$$

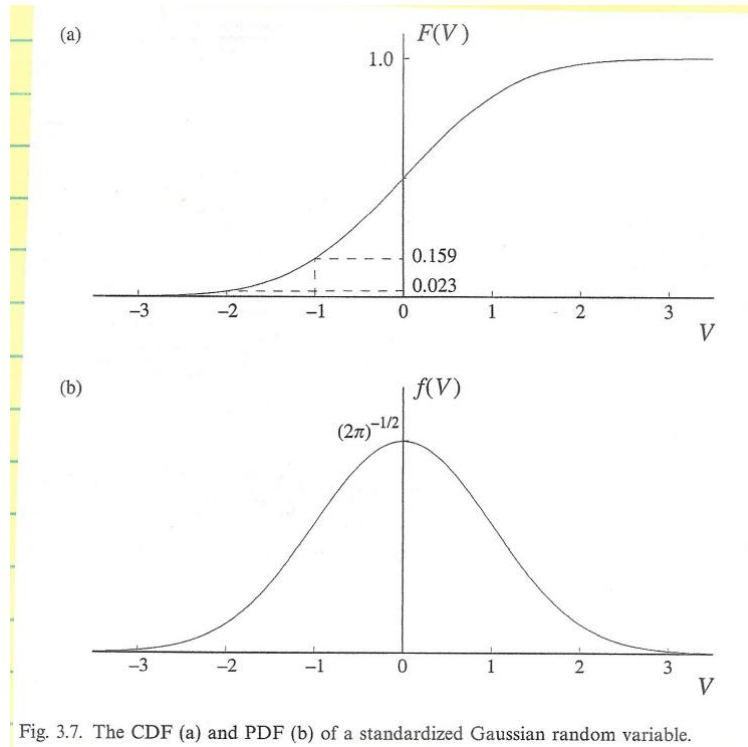


Fig. 3.7. The CDF (a) and PDF (b) of a standardized Gaussian random variable.